https://doi.org/10.5194/egusphere-2026-1763
Preprint. Discussion started: 26 May 2026

Global Ionospheric Response to the 17 March 2015 Geomagnetic Storm: A Multi-Station and Multi-Parameter Study

Lekshmi O Nair

St Berchmans College (Autonomous), Mahatma Gandhi University, Kerala, India

Correspondence to : lekshmikochuchira@gmail.com

Abstract

The global ionospheric response to the St. Patrick's Day Storm during 15–20 March 2015 is investigated using a comprehensive set of ground-based and satellite observations. Ionospheric parameters (foF2, hmF2, and h′F) from ionosonde stations distributed across different longitude sectors are analyzed in conjunction with geomagnetic field variations (H-component), thermospheric composition (O/N_2), and geomagnetic indices (Dst and Kp) to examine the coupled magnetosphere–ionosphere–thermosphere system.

During the main phase of the storm (17 March), a pronounced uplift of the F-region is observed at equatorial and low-latitude stations in both western and eastern longitude sectors, indicating the presence of enhanced eastward prompt penetration electric fields (PPEF). The associated increase in hmF2 and h′F, followed by enhancement in foF2, confirms the occurrence of a positive ionospheric storm driven by storm-time electrodynamics. The H-component exhibits a significant decrease across all stations, reflecting the intensification of the ring current, while enhanced fluctuations at higher latitudes indicate the contribution of auroral electrojets and field-aligned currents.

The thermospheric response, characterized by variations in the O/N_2 ratio, shows depletion during the main phase due to storm-time upwelling, followed by a marked increase during the recovery phase (18–19 March), indicating a transition toward an oxygen-rich thermosphere. This compositional change contributes to reduced recombination rates and sustained enhancement in electron density. The evolution of the equatorial electric field further reveals a transition from PPEF-dominated dynamics during the main phase to disturbance dynamo electric field (DDEF) effects during the recovery phase.

https://doi.org/10.5194/egusphere-2026-1763
Preprint. Discussion started: 26 May 2026

Overall, the results demonstrate that the ionospheric response to the storm is governed by a combination of prompt electrodynamic forcing and delayed thermospheric processes, with global coherence across longitude sectors and modulation by latitude and local time.

Keywords

Geomagnetic storm, Ionosphere, PPEF, DDEF, O/N_2 ratio, Equatorial electrodynamics, St. Patrick's Day Storm 2015.

1. Introduction

Geomagnetic storms represent one of the most significant drivers of variability in the near-Earth space environment, resulting from enhanced solar wind–magnetosphere coupling during disturbed solar conditions. These storms are typically initiated by the arrival of interplanetary coronal mass ejections (CMEs) or high-speed solar wind streams, which lead to intensified magnetospheric convection and energy deposition into the high-latitude ionosphere (Gonzalez et al., 1994; Tsurutani et al., 2006). The consequent disturbances propagate through the coupled magnetosphere–ionosphere–thermosphere system, producing complex and highly variable responses in ionospheric density, composition, and electrodynamics.

At low and equatorial latitudes, the ionospheric response to geomagnetic storms is primarily governed by storm-time electric fields and thermospheric dynamics. Two key electrodynamic processes are known to dominate: prompt penetration electric fields (PPEF) and disturbance dynamo electric fields (DDEF). PPEFs arise from rapid changes in magnetospheric convection driven by southward interplanetary magnetic field (IMF Bz) and can penetrate to low latitudes with minimal shielding, producing immediate and global ionospheric responses (Kelley et al., 2003; Fejer et al., 2007). In contrast, DDEFs are generated by storm-time thermospheric winds driven by high-latitude Joule heating and particle precipitation, leading to delayed and longer-lasting modifications in the ionospheric electric field (Blanc and Richmond, 1980; Fuller-Rowell et al., 1994).

The F-region ionosphere exhibits significant structural changes during geomagnetic storms, often characterized by vertical plasma redistribution and variations in peak electron density. The uplift

https://doi.org/10.5194/egusphere-2026-1763
Preprint. Discussion started: 26 May 2026

of the F-layer, reflected in increases in *hmF2* and *h'F*, is primarily driven by enhanced eastward electric fields through upward E×B drift, which can result in a positive ionospheric storm due to reduced recombination at higher altitudes (Prölss, 1995; Buonsanto, 1999). Conversely, storm-time thermospheric composition changes, particularly variations in the atomic-to-molecular ratio (O/N_2), play a crucial role in controlling ionospheric density by modulating recombination rates. A decrease in O/N_2 due to thermospheric upwelling leads to enhanced recombination and negative storm effects, whereas an increase during the recovery phase supports positive storm conditions (Rishbeth and Müller-Wodarg, 2006).

The geomagnetic field response during storms, commonly represented by the Dst index and ground-based H-component measurements, reflects the development of the ring current and associated current systems. A significant decrease in the H-component is indicative of ring current intensification, while superimposed short-term fluctuations are associated with auroral electrojets and field-aligned currents (Daglis et al., 1999; Kamide et al., 1998). These current systems play a critical role in coupling high-latitude energy inputs to low-latitude ionospheric dynamics.

The St. Patrick's Day Storm, which occurred on 17 March 2015, is one of the most intense geomagnetic storms of solar cycle 24, with a minimum Dst of approximately −223 nT. This event has been widely studied due to its pronounced global ionospheric and thermospheric impacts, including significant modifications in electron density, electric fields, and neutral composition (Astafyeva et al., 2015; Nayak et al., 2016). The storm provides an excellent opportunity to investigate the interplay between electrodynamic and thermospheric processes across different latitude and longitude sectors.

Although several studies have examined the ionospheric response to this event, most analyses are limited to specific regions or individual parameters. A comprehensive, multi-parameter investigation combining ionospheric, geomagnetic, and thermospheric observations across multiple longitude sectors remains limited. In particular, the role of longitudinal variability and local time modulation in shaping the global ionospheric response requires further investigation.

In this context, the present study aims to examine the global ionospheric response to the March 2015 geomagnetic storm using observations from multiple stations distributed across western and eastern longitude sectors. By integrating ionosonde measurements, geomagnetic field data, thermospheric composition, and satellite-derived electron density profiles, this study seeks to (1) characterize the temporal evolution of ionospheric parameters during different storm phases, (2)

https://doi.org/10.5194/egusphere-2026-1763
Preprint. Discussion started: 26 May 2026

identify the dominant electrodynamic processes controlling the response, and (3) assess the role of longitudinal and latitudinal variability in modulating storm-time ionospheric dynamics.

Unlike previous studies, which primarily focus on regional or single-parameter analyses, the present work provides a comprehensive multi-parameter investigation of the storm-time ionospheric response by integrating ionospheric, geomagnetic, and thermospheric observations across both western and eastern longitude sectors. The study highlights the global coherence of prompt penetration electric fields and quantifies the role of longitudinal and local time variability in modulating the ionospheric response.

2. Data and Methodology

The present study focuses on the intense geomagnetic disturbance associated with the St. Patrick's Day Storm during 15–20 March 2015. The storm was initiated by the arrival of an interplanetary coronal mass ejection (CME) at ~14:00 UT on 15 March 2015, followed by a prolonged southward turning of the interplanetary magnetic field (IMF Bz), reaching values of approximately −30 nT. This facilitated enhanced dayside magnetic reconnection and intensified magnetospheric convection.

The storm reached its peak intensity on 17 March, with the Dst index attaining a minimum value of ~−223 nT, indicating a severe geomagnetic storm (G4 level). The corresponding decrease in the H-component reflects the development of a strong ring current, while short-term fluctuations are associated with ionospheric current systems.

For analysis, the storm interval is categorized into three phases: initial phase (15 March 2015, ~14:00 UT), main phase (17 March 2015), and recovery phase (18–19 March 2015).

A combination of ground-based and satellite observations is utilized to examine the coupled magnetosphere–ionosphere–thermosphere system. The ionospheric parameters *foF2*, *hmF2*, and *h'F* are obtained from the Global Ionospheric Radio Observatory (GIRO). Here, *foF2* represents

https://doi.org/10.5194/egusphere-2026-1763
Preprint. Discussion started: 26 May 2026

the critical frequency proportional to peak electron density (NmF2), *hmF2* denotes the height of maximum electron density (km), and *h'F* indicates the virtual height associated with rapid vertical plasma motion.

The thermospheric composition is characterized using the O/N_2 ratio derived from the Global Ultraviolet Imager (GUVI) onboard the TIMED satellite. The O/N_2 ratio serves as an indicator of neutral composition changes that influence ionospheric recombination processes. The horizontal component (H) of the geomagnetic field is obtained from ground-based magnetometer stations provided by the INTERMAGNET. These data are used to examine storm-time variations associated with ring current development and ionospheric current systems. Global geomagnetic activity is characterized using the Dst and Kp indices obtained from the World Data Center for Geomagnetism Kyoto. Where Dst represents the intensity of ring current and Kp index indicates the planetary scale geomagnetic disturbances. To examine the global and longitudinal characteristics of storm-time ionospheric response, data from seven stations are selected and grouped into two longitude sectors: western longitudinal sector (American sector) and eastern longitude sector (Asian- African sector), This classification enables the investigation of longitudinal differences in ionospheric response, particularly those arising from local time dependence of electrodynamic processes.

The analysis is carried out using a multi-parameter and multi-station approach. Temporal variations of ionospheric parameters (*foF2*, *hmF2*, *h'F*), geomagnetic field (H-component), O/N_2 ratio, and geomagnetic indices are examined over the storm period in Universal Time (UT). Storm-time observations are compared with corresponding quiet-day conditions ($Kp \leq 2$) to isolate storm-induced disturbances.

Electrodynamic signatures are identified using variations in F-region parameters: increases in *hmF2* and *h'F* indicate eastward electric fields (upward E×B drift), while decreases indicate westward electric fields (downward drift). The observed variations are interpreted in conjunction

https://doi.org/10.5194/egusphere-2026-1763
Preprint. Discussion started: 26 May 2026

with IMF Bz, Dst, and Kp indices to identify the role of prompt penetration electric fields (PPEF) and disturbance dynamo electric fields (DDEF). Latitudinal and longitudinal analyses are performed to distinguish between global electrodynamic effects and localized thermospheric processes.

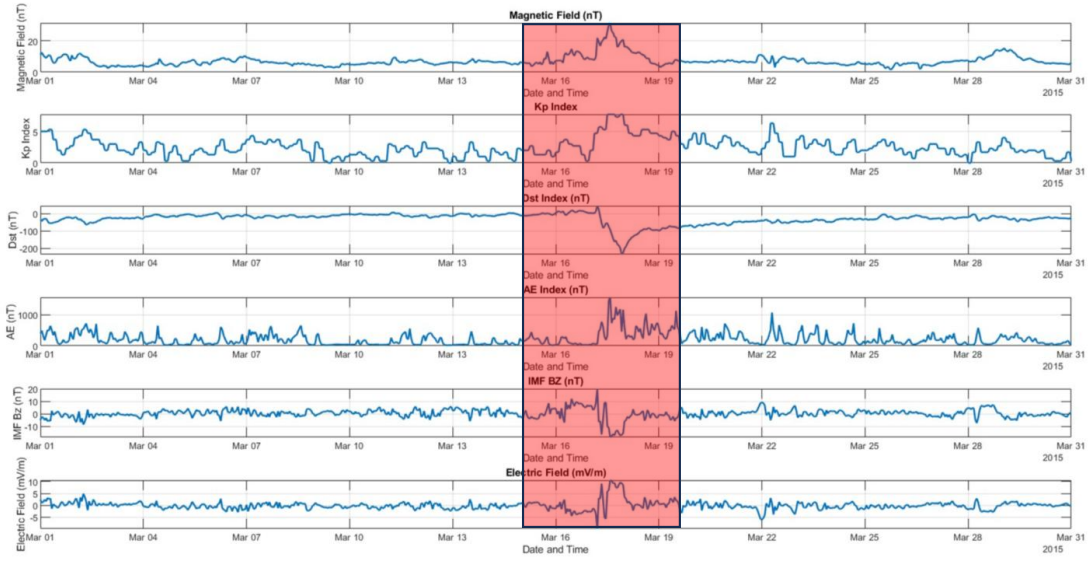

Figure 1. Temporal variations of geomagnetic indices (Dst and Kp), IMF Bz, and H-component during 15–20 March 2015. The shaded region highlights the main phase of the storm. The sharp southward turning of IMF Bz and corresponding decrease in Dst indicate the onset of intense geomagnetic activity.

A key feature observed during the main phase is the simultaneous disturbance at ~06:50 UT across all stations, including Yakutsk, Beijing, Guam, Jicamarca, Fortaleza, Hermanus, and Port Stanley. This near-simultaneity across a wide longitudinal sector indicates the penetration of magnetospheric electric fields to low latitudes, characteristic of prompt penetration electric fields (PPEF).

https://doi.org/10.5194/egusphere-2026-1763
Preprint. Discussion started: 26 May 2026

The immediate ionospheric response is manifested as abrupt variations in hmF2 and h′F, indicating rapid vertical plasma redistribution.

3. Results and Discussions

At equatorial and low-latitude stations within the western longitude sector, namely Jicamarca and Fortaleza, along with the southern high-latitude station Port Stanley, a pronounced storm-time disturbance is observed during the main phase.

At the equatorial and low-latitude stations, a clear uplift of the F-region is evident, manifested as a near-simultaneous increase in hmF2 and h′F around ~06:50 UT on 17 March 2015. This rapid uplift indicates the presence of an enhanced eastward electric field associated with prompt penetration electric fields (PPEF), which drives upward E×B drift.

The vertical transport of plasma to higher altitudes reduces recombination rates, resulting in a subsequent enhancement of foF2, characteristic of a positive ionospheric storm. The coherent response between Jicamarca and Fortaleza confirms the strong influence of storm-time electrodynamics in the equatorial region.

In contrast, the response at Port Stanley exhibits comparatively larger variability, reflecting the combined influence of electrodynamic processes and high-latitude energy inputs such as particle precipitation and Joule heating. Despite these differences, the simultaneous disturbance across the western sector indicates that the initial ionospheric response is driven by a globally coherent penetration electric field, with latitude-dependent modulation.

https://doi.org/10.5194/egusphere-2026-1763
Preprint. Discussion started: 26 May 2026

176 2 (a) 2(b)

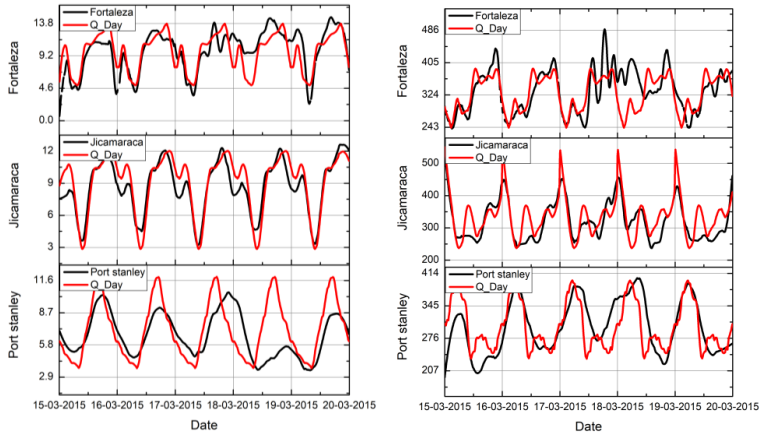

177

178 2(c)

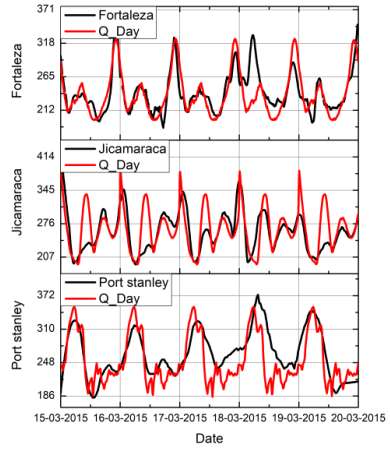

179

180 Figure 2.Temporal variations of ionospheric parameters (a) foF2,(b) h'F and (C) hmF2 during
181 storm and quiet conditions at Western Longitude Sector (American sector) (Fortaleza, Jicamarca,
182 and Port Stanley) for 15–20 March 2015.

https://doi.org/10.5194/egusphere-2026-1763
Preprint. Discussion started: 26 May 2026

During the later phase (~15 UT on 17 March), a reversal to westward electric fields is inferred from the downward movement of the F-region. This leads to suppression of the pre-reversal enhancement (PRE), a key driver of equatorial plasma instabilities. The inhibition of PRE indicates unfavorable conditions for the development of equatorial spread-F during this interval.

Overall, the equatorial and low-latitude ionospheric response during the storm is predominantly controlled by storm-time electrodynamics, with PPEF governing the initial uplift and subsequent electric field reversal modulating the evening ionospheric dynamics.

3(a)

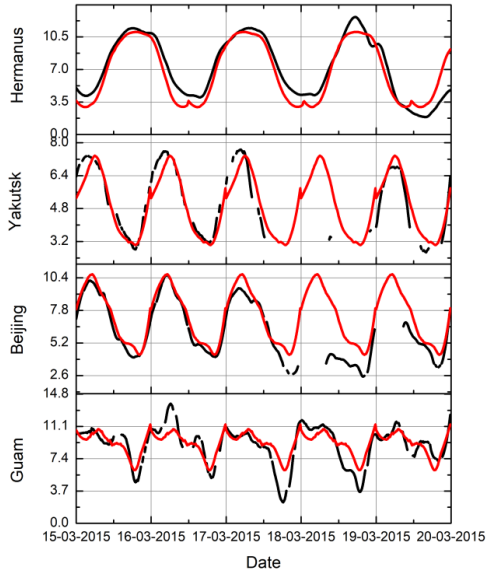

https://doi.org/10.5194/egusphere-2026-1763
Preprint. Discussion started: 26 May 2026

196 3(b)

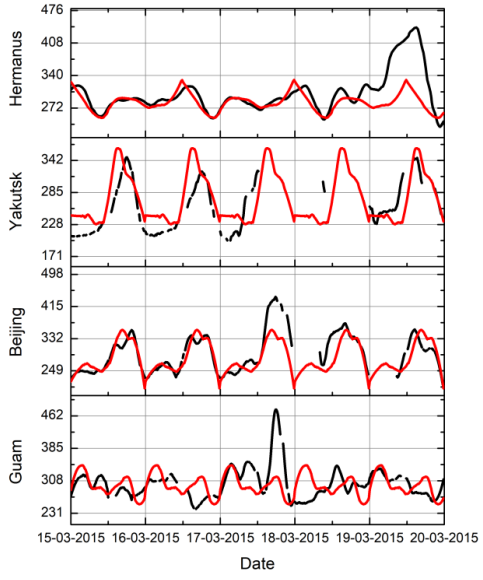

197

198 3(c)

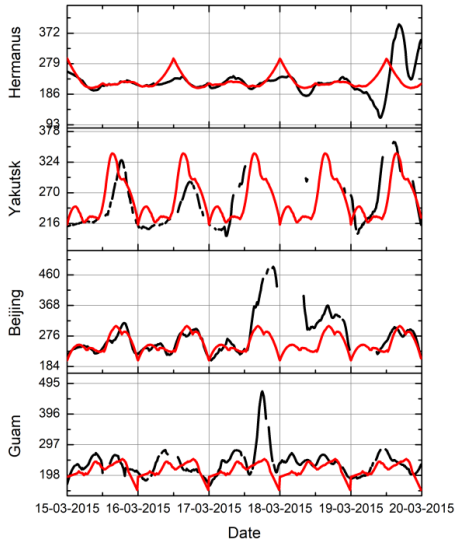

199

https://doi.org/10.5194/egusphere-2026-1763
Preprint. Discussion started: 26 May 2026

Figure 3. Temporal variations of ionospheric parameters (a) foF2, (b) h'F and (c) hmF2 during storm-time and quiet-day conditions at the Eastern Longitude Sector (Asian–African sector) (Yakutsk, Beijing, Guam, and Hermanus) for 15–20 March 2015.

The variations in the horizontal component (H) of the geomagnetic field clearly capture the evolution of storm-time magnetospheric and ionospheric current systems during the St. Patrick's Day Storm. The multi-station observations reveal both global signatures of ring current development and localized effects associated with ionospheric and auroral processes.

In the Western longitude sector (American sector) Jicamarca, Fortaleza, and Port Stanley a pronounced decrease in the H-component is observed during the main phase (17 March), consistent with the intensification of the storm-time ring current. The depletion is relatively smooth at the low- and equatorial-latitude stations (Jicamarca and Fortaleza), reflecting the dominant influence of the symmetric ring current.

In contrast, the response at Port Stanley exhibits enhanced fluctuations superimposed on the main depression. These rapid variations are indicative of high-latitude processes, including auroral electrojet activity, particle precipitation, and intensified Joule heating. This highlights the transition from globally driven magnetospheric currents at low latitudes to locally driven electrodynamic processes at higher latitudes.

In the Eastern longitude sector (Asian–African sector)—Yakutsk, Beijing, Guam, and Hermanus—a comparable large-scale decrease in the H-component is observed, confirming the global development of the ring current system. However, the temporal evolution and amplitude of the disturbance show noticeable variability across stations.

At higher latitudes, particularly at Yakutsk and Hermanus, the H-component exhibits strong irregular fluctuations, reflecting the influence of auroral current systems and field-aligned currents. At mid- and low-latitude stations such as Beijing and Guam, the response is

https://doi.org/10.5194/egusphere-2026-1763
Preprint. Discussion started: 26 May 2026

comparatively smoother, dominated by large-scale magnetospheric currents with limited local perturbations.

The simultaneous decrease in the H-component across both longitude sectors during the main phase indicates the global enhancement of the ring current, driven by sustained southward IMF Bz and enhanced magnetospheric convection. Superimposed short-term perturbations, particularly at higher latitudes, highlight the role of auroral electrojets, ionospheric currents, and field-aligned current systems.

Overall, the observations demonstrate that while the ring current produces a globally coherent depression in the H-component, the superimposed variability is strongly latitude-dependent and modulated by local electrodynamic processes, with minimal longitudinal dependence in the large-scale structure.

https://doi.org/10.5194/egusphere-2026-1763
Preprint. Discussion started: 26 May 2026

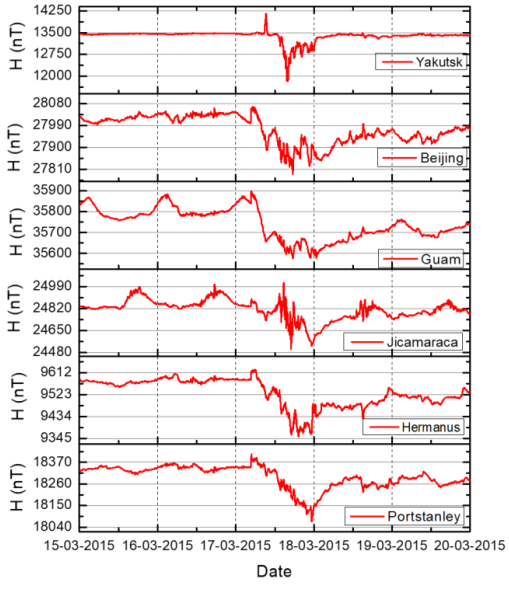

Figure:4 Temporal variations of the horizontal component (H) of the geomagnetic field at multiple stations during 15–20 March 2015.

The thermospheric composition, represented by the O/N_2 ratio, exhibits significant variability during the storm period and plays a crucial role in modulating ionospheric density through changes in recombination rates.

During the main phase (17 March 2015), a decrease in O/N_2 is inferred, particularly at mid- and high-latitudes, indicating an enhancement of molecular species (N_2 and O_2) driven by storm-time thermospheric upwelling. This compositional disturbance leads to increased recombination rates and contributes to the observed negative ionospheric storm effects, especially at stations in both longitude sectors.

In the Western longitude sector (American sector)—Jicamarca, Fortaleza, and Port Stanley—the recovery phase (18 March) is characterized by a marked increase in O/N_2, particularly at low and

https://doi.org/10.5194/egusphere-2026-1763
Preprint. Discussion started: 26 May 2026

equatorial latitudes. This enhancement indicates a transition toward an oxygen-rich thermosphere, reducing recombination rates and facilitating an increase in electron density. The effect is most evident at Jicamarca and Fortaleza, where the positive ionospheric storm response is more pronounced.

In the Eastern longitude sector (Asian–African sector)—Yakutsk, Beijing, Guam, and Hermanus—a similar recovery-phase enhancement in O/N_2 is observed, although with slight temporal differences across stations. These variations can be attributed to longitudinal differences in thermospheric circulation, driven by high-latitude energy input and subsequent equatorward propagation of disturbed neutral winds.

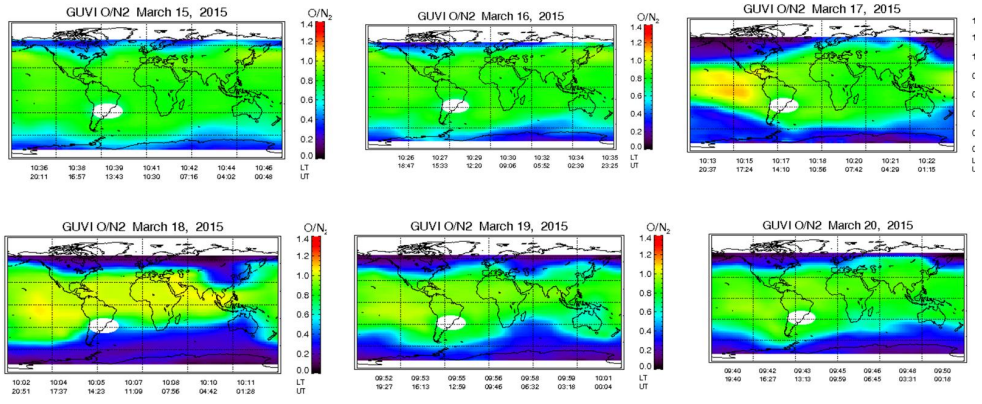

Figure:5 Temporal variations of the thermospheric O/N_2 ratio during 15–20 March 2015 over multiple locations, including Jicamarca, Fortaleza, Port Stanley, Yakutsk, Beijing, Guam, and Hermanus.

Overall, the O/N_2 variations indicate that thermospheric composition changes dominate during the recovery phase, contributing significantly to the positive ionospheric storm effect, while their influence during the main phase is secondary to electrodynamic forcing. The recovery-phase enhancement in O/N_2 is temporally consistent with the observed increase in foF2, confirming the dominant role of thermospheric composition in driving positive ionospheric storm effects

https://doi.org/10.5194/egusphere-2026-1763
Preprint. Discussion started: 26 May 2026

The equatorial electric field (EEF), inferred from the temporal variations in hmF2 and h′F, exhibits distinct signatures corresponding to storm-time electrodynamic processes and plays a dominant role in controlling the low-latitude ionospheric response.

During the main phase (~06:50 UT on 17 March 2015), a clear enhancement of the eastward electric field is observed simultaneously across both longitude sectors. This is evidenced by the rapid uplift of the F-region at equatorial stations in the Western sector—Jicamarca and Fortaleza—and in the Eastern sector at Guam. The simultaneity of this response confirms the action of prompt penetration electric fields (PPEF), which are global in extent and rapidly transmitted from high to low latitudes.

The enhanced eastward EEF drives upward E×B drift, leading to a rapid increase in hmF2 and h′F, and subsequently contributing to the enhancement of foF2. This process is responsible for the observed positive ionospheric storm effect at low and equatorial latitudes during the initial stage of the main phase.

https://doi.org/10.5194/egusphere-2026-1763
Preprint. Discussion started: 26 May 2026

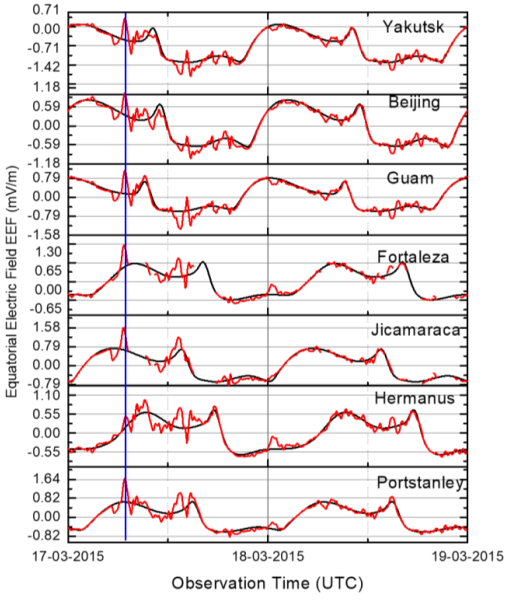

Figure:6 Temporal variations of the equatorial electric field (EEF) during 15–20 March 2015 at low- and equatorial-latitude stations, including Jicamarca, Fortaleza, and Guam.

During the later phase (~15 UT on 17 March), a reversal to westward electric fields is inferred from the observed downward movement of the F-region. This westward EEF suppresses the pre-reversal enhancement (PRE), thereby inhibiting the development of equatorial plasma instabilities. The consistency of this reversal across both longitude sectors indicates that the penetration of westward electric fields is also a globally coherent process.

In the recovery phase (18–19 March), the electric field is primarily governed by disturbance dynamo electric fields (DDEF), generated by storm-time thermospheric winds. The DDEF, typically eastward during nighttime, contributes to sustained uplift of the F-region and enhances electron density, particularly at low latitudes.

Although the primary features of EEF variation are consistent across both longitude sectors, minor differences in timing and magnitude can be attributed to local time dependence, which

https://doi.org/10.5194/egusphere-2026-1763
Preprint. Discussion started: 26 May 2026

modulates the efficiency of electrodynamic coupling and plasma transport. This transition from PPEF-dominated to DDEF-dominated electrodynamics highlights the temporal evolution of storm-time ionospheric forcing mechanisms.

4. Conclusion

The present study investigates the global ionospheric response to the St. Patrick's Day Stormduring 15–20 March 2015 using a combination of ground-based and satellite observations across multiple longitude sectors. The analysis reveals a complex interplay between magnetospheric forcing, ionospheric electrodynamics, and thermospheric composition.

During the main phase of the storm, a near-simultaneous uplift of the F-region is observed at equatorial and low-latitude stations in both longitude sectors, indicating the action of prompt penetration electric fields (PPEF). The associated enhancement in hmF2 and h′F, followed by an increase in foF2, confirms that storm-time electrodynamics plays a dominant role in driving the initial positive ionospheric response. The global coherence of this response highlights the rapid transmission of high-latitude electric fields to low latitudes.

The geomagnetic field variations show a pronounced decrease in the H-component across all stations, reflecting the development of a strong ring current during the main phase. Superimposed fluctuations at higher latitudes emphasize the contribution of auroral electrojets and field-aligned currents, demonstrating the combined influence of global and localized current systems.

Thermospheric composition, represented by the O/N_2 ratio, exhibits a depletion during the main phase due to storm-time upwelling, followed by a significant enhancement during the recovery phase. The increase in O/N_2, particularly at low and equatorial latitudes, reduces recombination rates and contributes to the sustained positive ionospheric storm effect.

The evolution of the equatorial electric field further illustrates the transition of dominant physical processes. While PPEF governs the initial phase through enhanced eastward electric fields and

https://doi.org/10.5194/egusphere-2026-1763
Preprint. Discussion started: 26 May 2026

upward plasma drift, a subsequent reversal to westward electric fields leads to suppression of the pre-reversal enhancement. During the recovery phase, disturbance dynamo electric fields (DDEF) become dominant, contributing to continued ionospheric uplift and delayed recovery.

Overall, the results demonstrate that the ionospheric response to the storm is governed by a combination of prompt electrodynamic forcing during the main phase and thermospheric composition changes coupled with disturbance dynamo effects during the recovery phase. The observed consistency across longitude sectors confirms the global nature of storm-time electrodynamics, while variations in magnitude and timing highlight the role of latitude and local time in modulating the response.

5. Data availability

The data used in this study are publicly available. TEC data were obtained from GIRO, Dst index data from the World Data Center for Geomagnetism, Kyoto, and Kp index data from the GFZ German Research Centre for Geosciences. FORMOSAT/COSMIC data were accessed from the CDAAC repository. All datasets are available from the respective data centers upon request or via their official websites.

6. Author contribution

The author confirms sole responsibility for the study conception and design, data collection, analysis and interpretation of results, and manuscript preparation.

7. .References

1. Blanc, M., Richmond, A.D., 1980. The ionospheric disturbance dynamo. *Journal of Geophysical Research* 85(A4), 1669–1686.
2. Buonsanto, M.J., 1999. Ionospheric storms—A review. *Space Science Reviews* 88, 563–601.

https://doi.org/10.5194/egusphere-2026-1763
Preprint. Discussion started: 26 May 2026

3. Daglis, I.A., Thorne, R.M., Baumjohann, W., Orsini, S., 1999. The terrestrial ring current: Origin, formation, and decay. *Reviews of Geophysics* 37(4), 407–438.
4. Fejer, B.G., Jensen, J.W., Su, S.-Y., 2007. Quiet time equatorial F region vertical plasma drift model derived from ROCSAT-1 observations. *Journal of Geophysical Research* 112, A11305.
5. Fuller-Rowell, T.J., Codrescu, M.V., Moffett, R.J., Quegan, S., 1994. Response of the thermosphere and ionosphere to geomagnetic storms. *Journal of Geophysical Research* 99(A3), 3893–3914.
6. Gonzalez, W.D., Joselyn, J.A., Kamide, Y., et al., 1994. What is a geomagnetic storm? *Journal of Geophysical Research* 99(A4), 5771–5792.
7. Kamide, Y., Baumjohann, W., Daglis, I.A., et al., 1998. Current understanding of magnetic storms: Storm-substorm relationships. *Journal of Geophysical Research* 103(A8), 17705–17728.
8. Kelley, M.C., Makela, J.J., Chau, J.L., Nicolls, M.J., 2003. Penetration of the solar wind electric field into the magnetosphere/ionosphere system. *Geophysical Research Letters* 30(4), 1158.
9. Prölss, G.W., 1995. Ionospheric F-region storms. In: Volland, H. (Ed.), *Handbook of Atmospheric Electrodynamics*, Vol. 2. CRC Press, Boca Raton, pp. 195–248.
10. Rishbeth, H., Müller-Wodarg, I.C.F., 2006. Why is there more ionosphere in January than in July? The annual asymmetry in the F2-layer. *Journal of Atmospheric and Solar-Terrestrial Physics* 68, 329–339.
11. Tsurutani, B.T., Gonzalez, W.D., Gonzalez, A.L.C., et al., 2006. Corotating solar wind streams and recurrent geomagnetic activity: A review. *Journal of Geophysical Research* 111, A07S01.

https://doi.org/10.5194/egusphere-2026-1763
Preprint. Discussion started: 26 May 2026

12. Astafyeva, E., Zakharenkova, I., Förster, M., 2015. Ionospheric response to the 2015 St. Patrick's Day storm: A global multi-instrumental overview. *Journal of Geophysical Research: Space Physics* 120, 9023–9037.

13. Nayak, C., Tsai, L.-C., Su, S.-Y., Galkin, I.A., 2016. Effects of the St. Patrick's Day geomagnetic storm on the low-latitude ionosphere. *Journal of Geophysical Research: Space Physics* 121, 786–801.

14.